Article:
Wei, D, Li, F, Wei, X et al. (3 more authors) (2020) Microstructure, nano-mechanical characterization, and fretting wear behavior of plasma surface Cr-Nb alloying on γ-TiAl. Proceedings of the Institution of Mechanical Engineers, Part J: Journal of Engineering Tribology. ISSN 1350-6501

https://doi.org/10.1177/1350650120939835

D.Wei, F.Li, X.Wei, T.Liskiewicz, K.Kubiak, P.Zhang, Microstructure nano-mechanical characterization and fretting wear behavior of plasma surface Cr-Nb alloying on gamma-TiAl, Proceedings of the Institution of Mechanical Engineers, Part J: Journal of Engineering Tribology 1-13 Copyright©2020 SAGE Publications. DOI: 10.1177/1350650120939835

Microstructure nano-mechanical characterization and fretting wear behavior of plasma surface Cr-Nb co-alloying on γ-TiAl

Dongbo Wei[a, d, e]*, Fengkun Li [a, d]*, Xiangfei Wei[a], Tomasz Liskiewicz[c], Krzysztof J. Kubiak[b], Pingze Zhang[a,d]

*corresponding.author, Dongbo Wei,weidongbo@nuaa.edu.cn; Fengkun Li, lifengkun@nuaa.edu.cn

[a] College of Materials Science and Technology, Nanjing University of Aeronautics and Astronautics, Nanjing,211106, China.

[b] School of Mechanical Engineering, University of Leeds, Leeds, LS2 9JT, UK

[c] Department of Engineering, Faculty of Science and Engineering, Manchester Metropolitan University, Manchester, M15 6BH, UK

[d] Materials Preparation and Protection for Harsh Environment Key Laboratory of Ministry of Industry and Information Technology, Nanjing,211106, China

[e] Aero-engine Thermal Environment and Structure Key Laboratory of Ministry of Industry and Information Technology, Nanjing, 211106, China

Abstract

In this study, surface Cr-Nb co-alloying was realized on γ-TiAl based on double glow plasma hollow cathode discharge effect. An inter-diffusion layer was detected under the surface, which mainly composed of Cr_2Nb intermetallic compounds. After Cr-Nb co-alloying, the surface nanohardness of γ-TiAl increased from 5.65 GPa to 11.61 GPa. The surface H/E and H^3/E^2 increased from 3.37 to 5.98 and increased from 0.64 to 4.15, respectively, which indicated the improvement of plastic deformation resistance of γ-TiAl after Cr-Nb co-alloying, and it was beneficial to the anti-fretting wear. Cr-Nb co-alloying coating and its effect on fretting wear property was investigated. The fretting wear test showed that the average friction coefficient of γ-TiAl with Si_3N_4 ball was significantly decreased after Cr-Nb co-alloying. The fluctuation of friction coefficient at the initial stage of friction was significantly improved. With the increase of friction cycle, the friction process of both γ-TiAl before and after Cr-Nb co-alloying could be divided into the formation of debris, flaking, formation of crack, delamination. However, the high hardness, resistance to plastic deformation and fatigue resistance of γ-TiAl after Cr-Nb co-alloying could

inhibit the formation of debris and delamination during friction test. The surface wear scar area and the maximum wear scar depth of γ-TiAl were decreased obviously, indicating the wear resistance of γ-TiAl has been greatly improved after Cr-Nb co-alloying. The results indicated that plasma surface Cr-Nb co-alloying was an effective way to improve the fretting wear resistance of γ-TiAl in aviation area.

Keywords: Cr-Nb co-alloying coating; Fretting wear; Double glow plasma surface metallurgy technology; γ-TiAl

1. Introduction

TiAl alloy has shown the promising application prospect in the manufacturing of high thrust-to-weight ratio aircraft engines due to its lower density and higher elastic modulus than nickel-base superalloy [1–3]. Some researches even called TiAl alloy as the new generation of high-temperature structural materials to replace nickel-base superalloy [4, 5]. It was reported that GEAE has applied TiAl alloy blades in the GE90 engine, reducing the weight by 200~300 kg. Airbus and Boeing have also respectively proposed research project on improving the engine's push ratio by using TiAl alloy blades at the rear of the low-pressure turbines [4].

There was no doubt that TiAl alloy was embracing a rising opportunity. However, TiAl alloy still has great distance from the clinical application. The main obstacles were big brittleness, poor wear resistance and high temperature oxidation resistance [5,6].The brittleness of TiAl alloy was related to its crystal structure. At room temperature, the slip system was insufficient due to the super dislocation was not easy to operate, which made the cleavage crack of TiAl alloy occurred and resulted in brittle fracture. Poor oxidation resistance of TiAl alloy was mainly due to the inability to form a protective alumina film at high temperature oxidation [7,8]. Due to the formation competition between Al and Ti during the oxidation process at high temperature, a mixed Al_2O_3/TiO_2 scales were formed. Intermixed oxides were less protective than continuous Al_2O_3 because the outward growth part of the oxide film was mainly rutile with porous structure. The inward part contained a mixture of α-Al_2O_3 and TiO_2, through which the external diffusion of Ti and the internal

diffusion of O transported rapidly [9,10].

In addition to poor high-temperature oxidation resistance, TiAl alloy had low surface hardness and poor bearing capacity, and showed serious wear. Usually, serious abrasive wear of TiAl alloy would happen under dry friction condition at room temperature. The poor wear resistance was another major drawback of TiAl alloy [11].

Alloying was an effective way to improve the wear and oxidation properties of TiAl alloy [12–14]. A number of studies indicated that alloying of Nb, Cr, Hf, Zr, W to TiAl alloy could increase the ductility and oxidation resistance, especially Nb could greatly improve the high temperature oxidation resistance of γ-TiAl [15,16]. The research of Zhao YB et al. showed that Nb could enhance the directionality of d-d bonds and the P-N stresses by dissolving in γ-TiAl phase, and then the critical resolved shear stress (CRSS) of ordinary dislocation slip was increased, which made TiAl alloy have higher strength and ductility [17]. Furthermore, Nb could improve the thermodynamic activity of Al and promote the formation of Al_2O_3 oxidation film. When Nb ions with valence electrons of +5 were added to titanium oxide, the concentration of oxygen vacancy would decrease, which may inhibit the growth of TiO_2 [18]. Recent research about high Nb containing TiAl alloys revealed that doped elements with higher valence than titanium (such as Nb) reduced oxygen vacancy concentration due to the electronneutrality of oxide, thus inhibiting the growth of TiO_2 [19,20]. The research of X. Lu et al. showed that the addition of Nb promoted the formation of TiN in oxidized oxide scale, promoted the formation of Nb enriched diffusion layer between scale and the substrate, and effectively prevented the diffusion of Ti and O ions [21]. High Nb-TiAl alloys were expected to be used in the temperature range of 800-900 °C. Nb could significantly improve not only the oxidation resistance of the TiAl alloy, but also their creep resistance, which exhibit distinctively balanced properties at high temperatures compared with traditional TiAl alloy. So Ti-Al-Nb alloys had been widely investigated in recent years [21]**.** Moreover, the addition of Nb could strength the γ-TiAl phase, and improve the hardness, which contribute to improve the wear resistance. The research of Adam et al reveal that Nb

would dissolve into γ-TiAl compound when the addition exceed 5.0 at.%, which played a role of grain refinement and solution strengthening, and led to the improvement of microhardness and wear resistance [22].

Cr could reduce the capital phase lattice constant line ratio (c/a), and improve the solution force and refine the grains, and importantly make the twin deformation more active at room temperature, resulting in the increasing of ductility [18]. In addition, the addition of Cr could inhibit the formation of nitrides at the initial stage of oxidation and promote the formation of Al_2O_3 oxidation film. In the meantime, the low oxygen permeability $Ti(Cr,Al)_2$ Laves phase formed during the oxidation process could effectively inhibit the internal diffusion of oxygen, and the protective Al_2O_3 oxidation film could be formed after the oxidation of Laves phase, which reduced the minimum Al content required for the formation of Al_2O_3 oxidation film. F. Wang et al found that when the Cr concentration was more than 10 at%, the high temperature oxidation resistance of TiAl was obviously improved [23]. Laska Nadine et al found that Cr promoted the formation of $(Ti,Nb)(Cr,Al)_2$ Laves which contributed to improve the oxidation resistance [23]. In previous studies of our research work, we prepared the Ni-Cr co-alloying coating on the γ-TiAl by double glow plasma surface alloying technique. Moreover, the oxidation and wear resistance of γ-TiAl were improved obviously [24,25].

Since wear and high temperature oxidation occurred on the surface of specimen, surface Cr or Nb alloying to a certain extent will be conducive to improve the oxidation resistance and wear resistance of TiAl alloy. In the meantime, the surface alloying avoided the reduction of the plasticity of TiAl alloy by overall Nb alloying. However, it was hard to realize surface Nb alloying on TiAl alloy. This was due to Nb has a melting point of up to 2400 ℃, which was great obstacle for surface Nb alloying.

The high energy density carrier, such as laser beam and plasma beam, provided possible technical approaches for surface Nb alloying on TiAl alloy. In previous study, we proposed the idea of plasma surface alloying on TiAl alloy and constructed the

enhanced plasma bombardment, sputtering and diffusion experimental device based hollow cathode glow discharge phenomenon [26]. And then, Cr-Nb co-alloying was successfully realized on γ-TiAl by plasma surface alloying device.

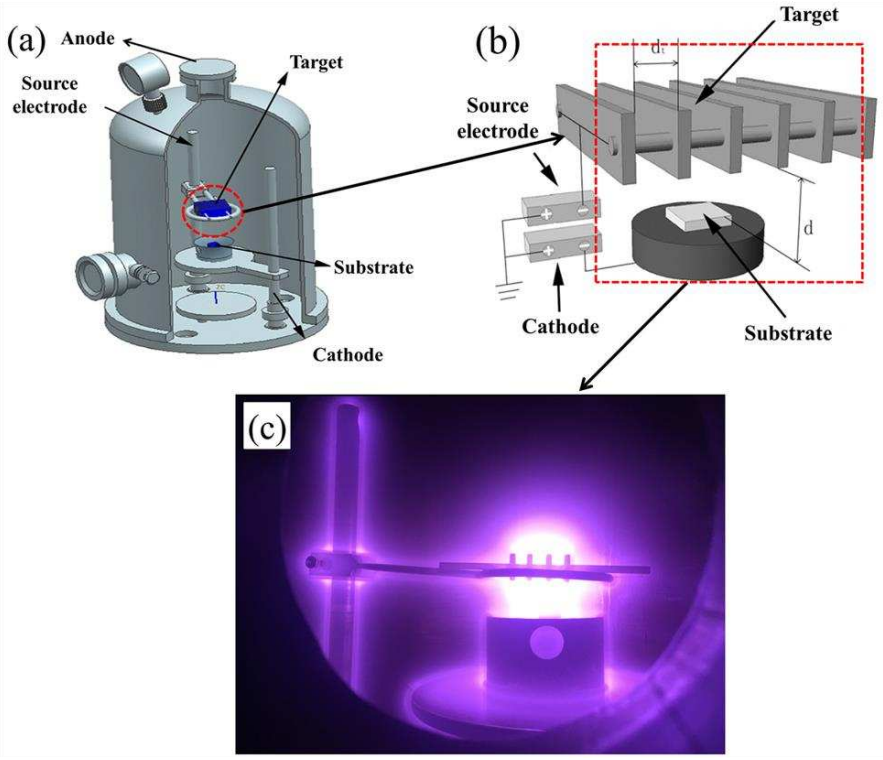

Fig.1 The schematic diagram of plasma surface Cr-Nb alloying on γ-TiAl

Fig.1 showed the experimental equipment and schematic diagram of plasma surface Cr-Nb alloying on γ-TiAl. The Cr-Nb target (Cr:Nb=20:80 at%) was fabricated into 80 mm×15 mm×5 mm sheet specimens by wire cut electrical discharge machining. Then 4-6 sheets of target were connected by alloy rods with the same composition as the target to form a grid hollow cathode source target. Target and γ-TiAl were placed in a sealed chamber, and a certain amount of argon was passed through the test process after vacuum extraction. The Cr-Nb target was connected to pulse power supplies, which will generate equipotential hollow cathode glow discharge between Cr-Nb sheets. Cr and Nb were sputtered from the target. In the meantime, the substrate electrode was connected to DC power supplies, which's potential was lower than the target's. The potential difference between substrate and

target would result in unequal potential hollow cathode glow discharge between substrate and target. It would heat γ-TiAl to 900~950 ℃. In the meantime, Cr and Nb sputtered from the target would deposit and diffuse on the surface of γ-TiAl under unequal potential hollow cathode effect. By adjusting the distance between the source and substrate, voltages of the target and γ-TiAl, argon pressure and other process parameters, a continuous and stable "equipotential+unequal potential" hollow cathode glow discharge phenomenon will be stable for several hours, as shown in Fig.1(c). After 3~5 hours processing, a Cr-Nb co-alloying coating will be eventually formed on the surface of γ-TiAl.

In the process, plasma bombardment activated the surface of γ-TiAl, which was very beneficial for Nb alloying. At the same time, Nb was distributed in the plasma with the form of charged particle groups and individual atoms. It improved Nb's diffusion capability. Isothermal temperature oxidation test in air showed that after plasma Cr-Nb co-alloying, the oxidation resistance of γ-TiAl at 750-950 ℃ was significantly enhanced. A continuous protective oxide film with Al_2O_3 and Cr_2O_3 was observed, which was very beneficial to oxidation resistance.

However, while improving the resistance to high temperature oxidation, the improvement of γ-TiAl's resistance to fretting wear could not be ignored. It was well know that fretting wear damage was easy to occur between the blades and the turbine disc of engine blade due to the change of vibration load of aero engine, as shown in Fig. 2 [27].

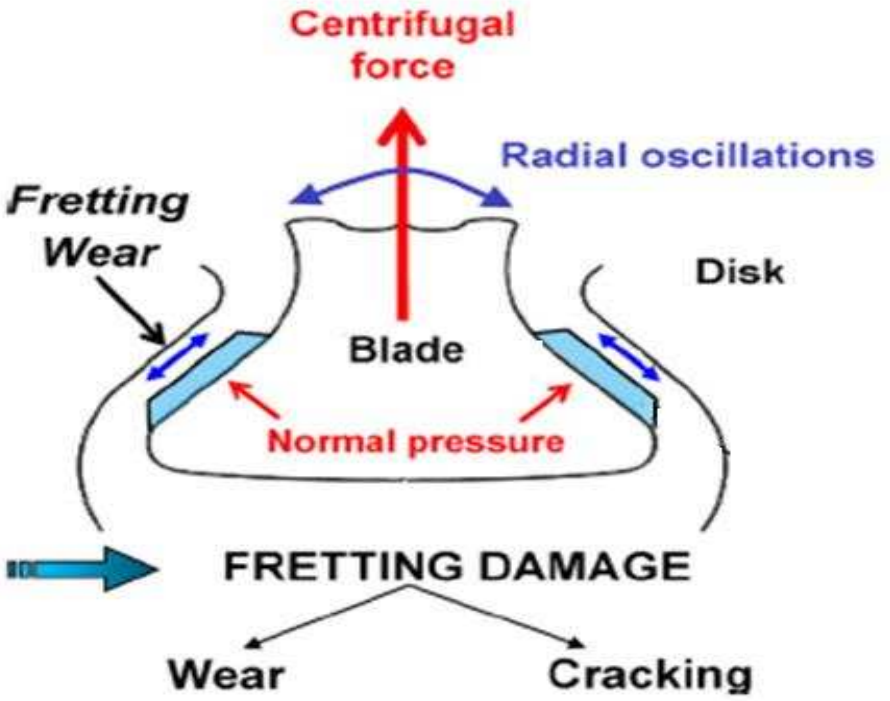

Fig. 2 Schematic diagram of fretting wear between blade mortise and turbine disc under working conditions

Previous study have shown that the wear resistance of TiAl alloy was worse than that of nickel base alloy [28]. That was to say, there was a greater risk of fretting wear between the blades made of γ-TiAl and the turbine disc. Actually, the TiAl alloy blade was always faced with the threat of fretting fatigue and wear at the junction of the blade mortise and turbine disk under high rotating speed.

In previous study，after plasma surface Cr-Nb co-alloying, the micro-hardness of γ-TiAl was effectively enhanced. Increasing the hardness could effectively improve the fretting wear resistance of γ-TiAl, which was also the development direction of advanced wear-resistant materials [29]. However, relevant studies showed that both hardness, mircro stress and plastic deformation resistance would affect fretting wear properties of γ-TiAl [30]. Therefore, the influence of Cr-Nb co-alloying on the micro-stress and plastic deformation resistance of γ-TiAl needed to be further studied, which benefitted to explain the mechanism of Cr-Nb co-alloying on the fretting wear performance of γ-TiAl.

The development of Nano mechanical properties characterization technique provided an effective method to characterize the micro-hardness, micro-stress and plastic deformation resistance of γ-TiAl before and after Cr-Nb co-alloying. During the Nano-indentation test, the pressing depth of the indenter was only micron or even nanometer, which could avoid the influence of the matrix on the test results and more accurately characterized the nano mechanical properties of the Cr-Nb co-alloying coating [31].

The purpose of this present work was to study the effect of plasma surface Cr-Nb co-alloying on fretting wear behavior of γ-TiAl. A Cr-Nb co-alloying was realized based on the hollow cathode effect generated by glow plasma discharge. SEM and XRD were used to analyze the morphology, composition and structure of the surface and cross section of the coating. The nano-hardness, elasticity modulus and plastic deformation resistance of the Cr-Nb co-alloying coating were measured by nano-indentor. Fretting wear behaviors of γ-TiAl before and after plasma surface Cr-Nb co-alloying under different cycles were studied in detailed by pin-on-plate fretting rig at room temperature.

2. Experimental details

2.1 Process of plasma surface Cr-Nb co-alloying on γ-TiAl

The substrate was γ-TiAl developed by Beijing Iron and Steel Research Institute in China. The specific chemical composition was shown in Table 1. Wire cut electrical discharge machining was used to process γ-TiAl into a square sample of 14 mm×14 mm×4 mm. SiC water sandpaper and metallographic sandpaper were used to polish the surface of the sample, and then used flannelette to polish the surface to a mirror. Finally, the polished samples were washed in acetone by ultrasonic for 5 minutes and dried.

Table 1 Chemical composition of γ-TiAl alloy (wt.%)

Ti	Al	V	Cr	Nb	O	C	N
Bal.	46.5	≦1.5	≦1	≦0.20	≦0.015	≦0.10	≦0.05

The target material was Cr-Nb alloy (Cr:Nb=20:80 at%) produced by Jiangxi

Ketai New Materials Co., Ltd. in China by powder metallurgy. The Cr-Nb target was fabricated into 80 mm×15 mm×5 mm sheet specimens by wire cut electrical discharge machining. Then 4 sheets of target were connected by alloy rods with the same composition as the target to form a grid hollow cathode source target. Argon (> 99.99%) was selected as working carrier gas in the experiment. The process parameters of plasma Cr-Nb co-alloying are presented in Table 2.

Table 2 Process parameters of the Cr-Nb co-alloying

Process parameters of the Cr-Nb co-alloying	Settings
distance between the source and substrate (mm)	19
voltage of the cathode (V)	550-600
voltage of the source electrode (V)	850-900
soaking time (h)	3
working pressure (Pa)	35
soaking temperature (℃)	918
spacing of target, d_t (mm)	15

2.2 Characterisation of Cr-Nb co-alloying

JSM-6360LV scanning electron microscopy (SEM) made in Japan was used to observe the morphology and structure of the surface and cross section of γ-TiAl before and after plasma surface Cr-Nb co-alloying. The composition and distribution of elements in different parts of the Cr-Nb co-alloying coating were analyzed by EDS.

Bruker D8-ADVANCE X-ray diffractometer (Cu target, sol-X detector, 40kV, 40mA, scanning speed 1-6 degree/min) was used to determine the phase composition of γ-TiAl after plasma surface Cr-Nb co-alloying.

Ultramicroscopic nanoindentation hardness tester manufactured by British Micro-materials Company was used in the experiment. The indenter was a diamond triangular cone indenter with a load of 100 mN and a holding time of 10 s. The loading speed was 1.32 mN/sec. Both the γ-TiAl surfaces before and after Cr-Nb co-alloying were polished to a mirror, and five different areas of theγ-TiAl surfaces before and after Cr-Nb co-alloying were selected for testing. Relevant research showed that H/E could be used to characterize the wear resistance of materials. And, H/E corresponded to the resistance of elastic strain to failure. H^3/E^2 corresponded to the plastic deformation resistance [32]. Therefore, in present study, H/E and H^3/E^2

were used to characterize the plastic deformation resistance and elastic strain to failure of the γ-TiAl before and after Cr-Nb co-alloying, so as to further explain the anti-fretting wear mechanism.

2.3 Fretting wear test

The fretting wear testing was carried out in a closed box at room temperature (20±1℃) and relative humidity of 60±5% without any lubrication conditions, as shown in Fig.3. The counter-body was Si_3N_4 balls with the diameter of 5 mm. Fretting friction test parameters were as follows: normal force: 30N, sliding frequency: 5Hz, displacement amplitude: 100 μm, total cycles: 2500-10000. Before testing, samples were polished to a mirror. At the beginning of the test, normal force (P) was applied on the surface of sample. And then, the real-time tangential force and relative displacement of the contact surface were recorded when the sample and the friction ball move reciprocally with a certain frequency and relative slip range. The tangential force (F_t) and the corresponding displacement (D) were measured and recorded every 1000 cycles in the process of test, and then drew the tangential force-displacement (F_t-D) curves. Furthermore, the maximum depth of the wear scar area and the morphology were measured by scanning electron microscopy (SEM) and NPFLEX 3D white light interferometer to evaluate the wear resistance. To ensure the accuracy of the test data, the micro-dynamic friction test was repeated three times for each parameter.

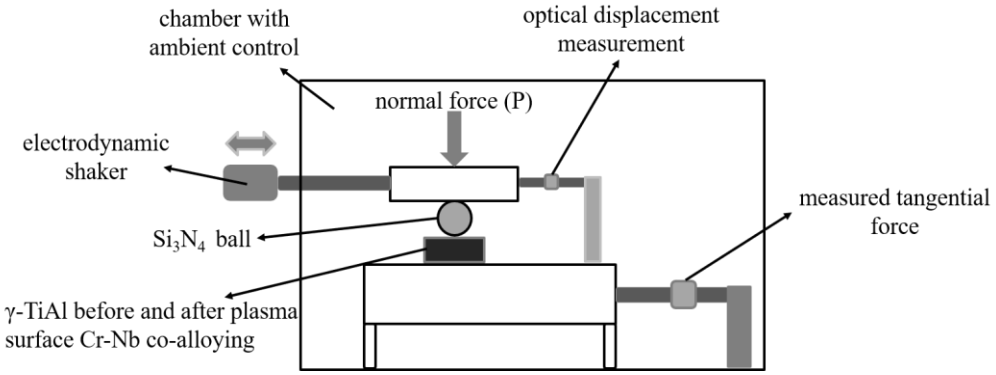

Fig.3 The schematic diagram of fretting friction equipment

3. Results

3.1 Microstructure characterization and phase compositions of γ-TiAl after plasma surface Cr-Nb co-alloying.

Fig. 4(a) showed the surface morphology of γ-TiAl after plasma surface Cr-Nb co-alloying. Some surface pits and humps were obvious on the surface, which were caused by the sputtering corrosion and particle packing under the effect of hollow cathode. It was worth noting that the ratio of chromium to niobium on the surface was very far from that of Cr-Nb target due to the difference of the sputtering rate between chromium and niobium in the plasma surface Cr-Nb co-alloying. Fig.4 (b) was the XRD pattern of γ-TiAl after plasma surface Cr-Nb co-alloying. The peak intensity of Cr_2Nb was even higher than Nb. It indicated that there were large amounts of Cr_2Nb intermetallic compounds formed.

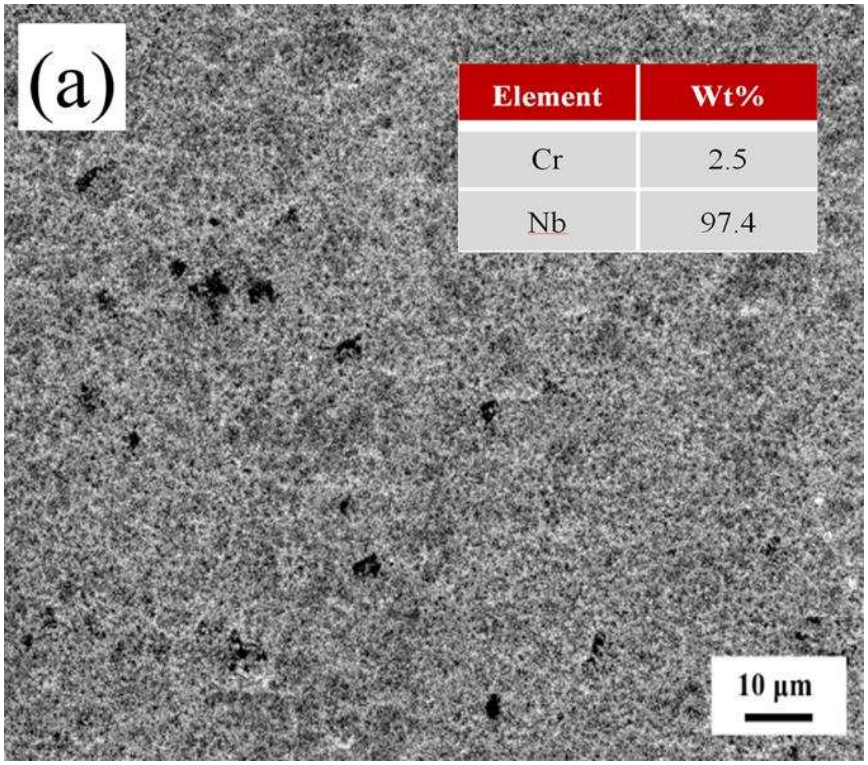

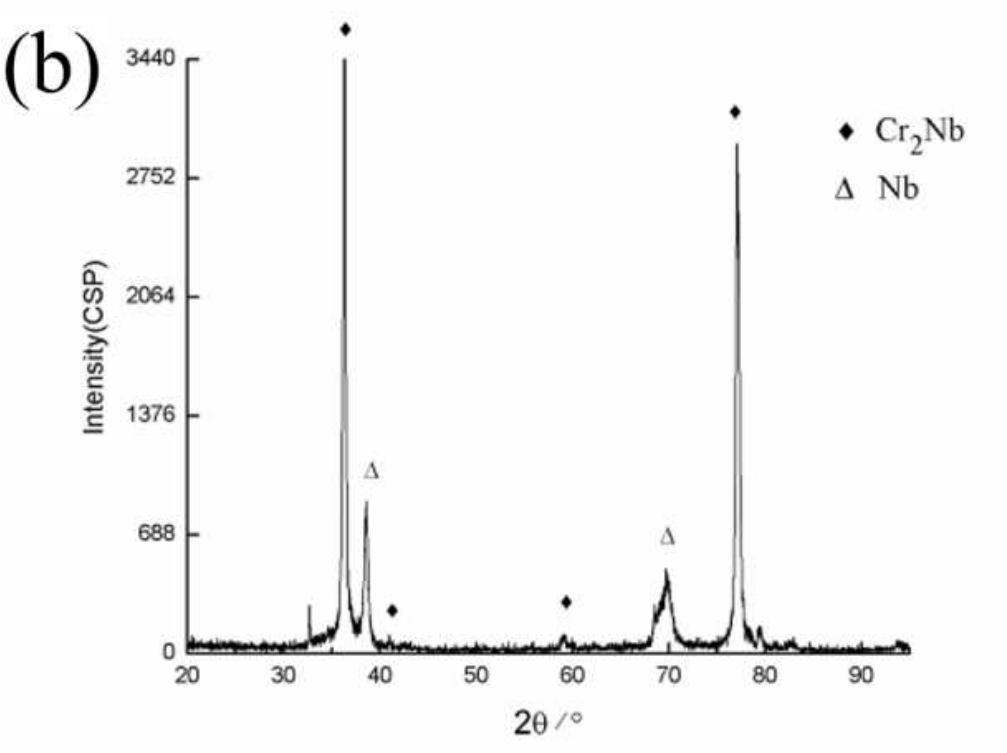

Fig.4 Surface morphology (a) and XRD pattern (b) of the Cr-Nb co-alloying coating

Fig. 5 showed cross-sectional morphology and component distribution of γ-TiAl after plasma surface Cr-Nb co-alloying. An obvious alloying layer was observed, whose thickness was about 15 μm, as shown in Fig. 5(a). The composition analysis along the surface depth direction indicated a 2 μm interdiffusion layer was formed under the deposition layer, as shown in Fig. 5(b). The elements were gradient distributed in the interdiffusion layer. The contents of Cr, Nb decreased gradually, but the contents of Ti, Al increased gradually.

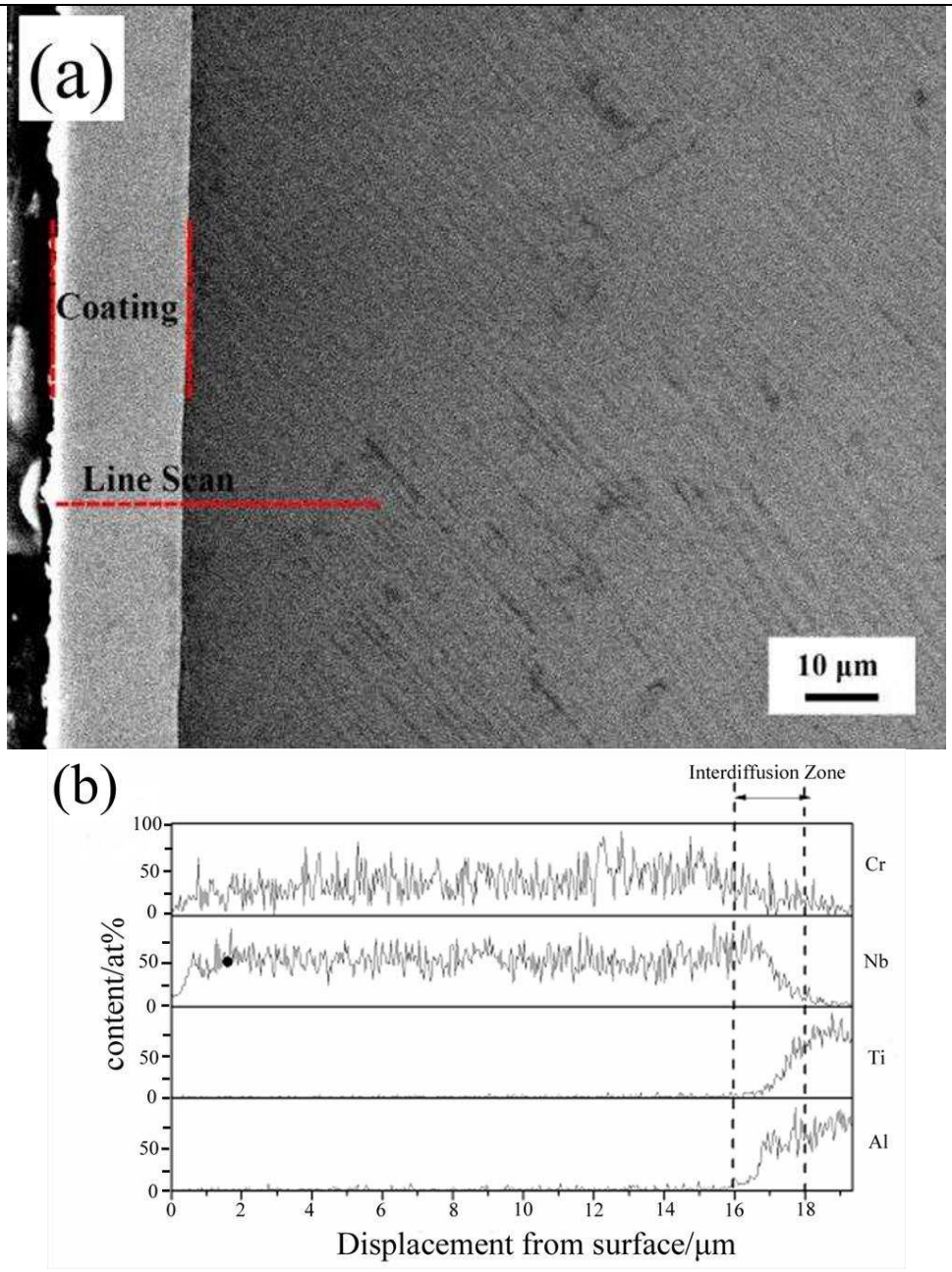

Fig. 5 Cross-sectional morphology (a) and EDS line scans (b) of γ-TiAl after plasma surface Cr-Nb co-alloying

From Fig.4 and Fig.5, it can be concluded that after Cr and Nb sputtered out from the target, they reacted on the surface of the γ-TiAl. Cr_2Nb intermetallic compounds were formed under the surface. In the meantime, an interdiffusion behavior of Cr, Nb and Ti, Al occurred under the high strength hollow cathode effect.

3.2 Nano-mechanical characterization

Fig. 6 showed the load-displacement curves of γ-TiAl before and after plasma

surface Cr-Nb co-alloying. As can be seen, under the same loading condition, the maximum indentation depth of the γ-TiAl was 0.90 μm, and the residual indentation depth after unloading was 0.65μm. In contrast, the maximum indentation depth of the Cr-Nb co-alloying coating was 0.67 μm, while the maximum residual depth after unloading was 0.39 μm. It indicated the Cr-Nb co-alloying improved the ability of γ-TiAl to resist plastic deformation.

When the indentation depth was greater than 300 nm, the alloyed sample's indentation depth was significantly lower than that of γ-TiAl substrate under the same load. When the load reached 100 mN, the indentation depth of γ-TiAl after Cr-Nb co-alloying was decreased from 910 nm to 640 nm. It indicated that plasma surface Cr-Nb co-alloying significantly enhanced the microplastic deformation resistance of γ-TiAl [31].

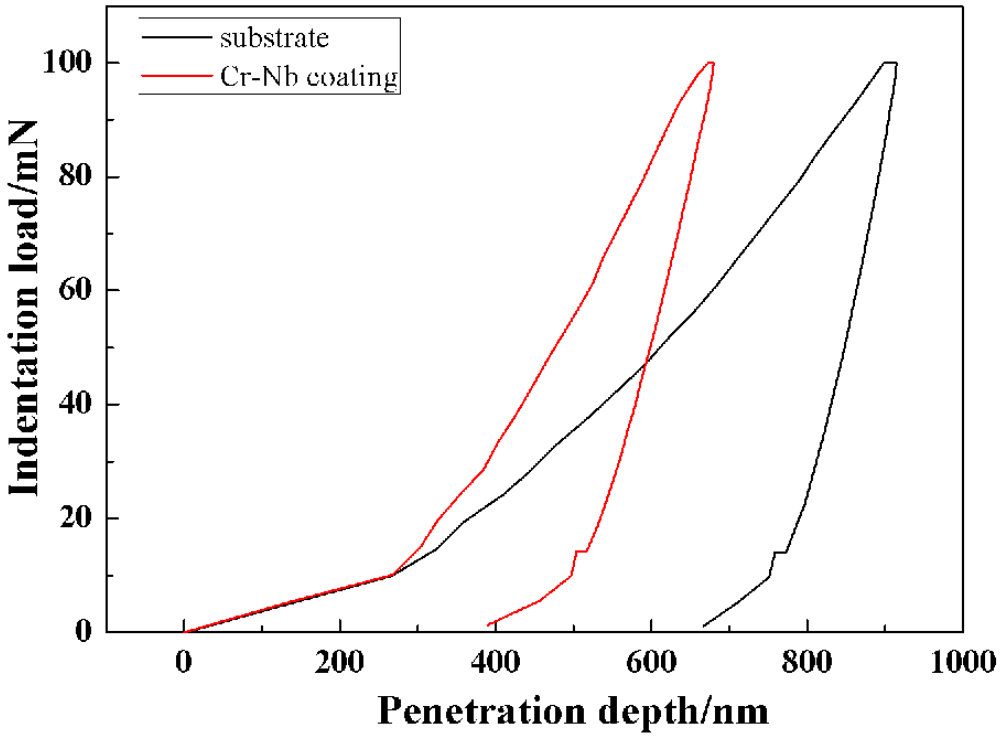

Fig. 6 Load–displacement curves of γ-TiAl before and after plasma surface Cr-Nb co-alloying

Research showed that metals and alloys exhibited an obvious creep behavior during the holding stage of nano-indentation test [33]. This referred to the phenomenon that the indentation depth increased when the load remained constant. In

this study, it was worth noting that the creep deformation of γ-TiAl was greatly inhibited after plasma Cr-Nb co-alloying in the holding stage. This indicated that plasma surface Cr-Nb co-alloying was also beneficial to the surface creep deformation resistance of γ-TiAl to microstress.

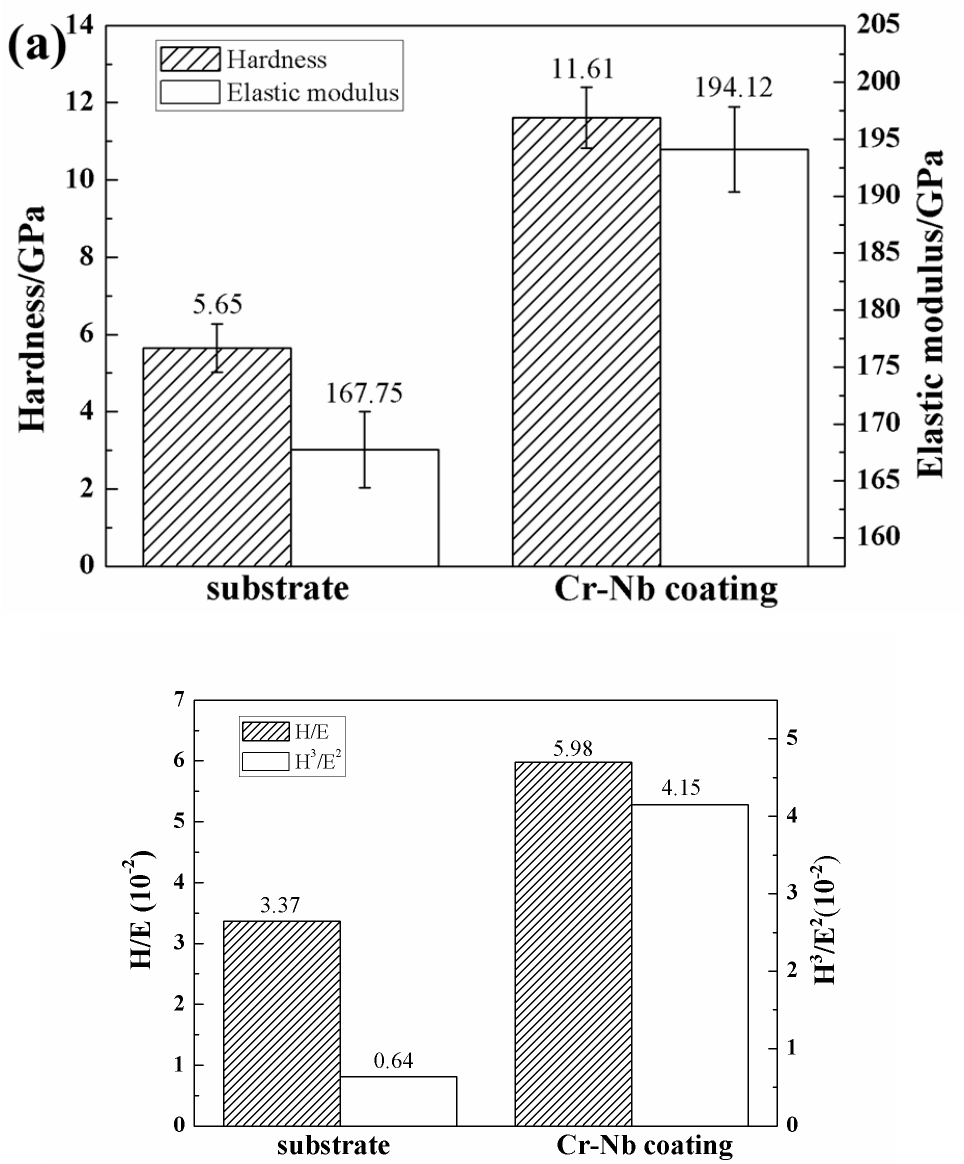

Fig.7 The hardness, elastic modus (a) and H/E, H^3/E^2 (b) of γ-TiAl before and after plasma surface Cr-Nb co-alloying

In the load-displacement curve, the slope of the unloading curve reflected the elastic deformation capacity of the specimen. During unloading stage, the slope of unloading curve of γ-TiAl shows decreased after plasma surface Cr-Nb co-alloying.

That was to say, the elastic rebound of γ-TiAl at unloading stage increased after co-alloying. It indicated that plasma surface Cr-Nb co-alloying enhanced the microelastic deformation resistance of γ-TiAl.

The area surrounded by the loading-unloading curves was characterized by the plastic deformation work of the specimen during the loading and unloading process, which represents the amount of plastic deformation of the specimen [31]. As shown in Fig. 6, the encircled area of load-unload curve of the Cr-Nb co-alloyed sample was much smaller than that of γ-TiAl substrate. It indicated that the Cr-Nb co-alloying coating had higher resistance to plastic deformation and lower adhesion transfer between contact surfaces of substrate and wear ball. Relevant studies showed that lower adhesion between contact surfaces of substrate and wear ball was beneficial to improving fretting wear properties of materials, which indicated that the fretting wear resistance of Cr-Nb co-alloying coating was better than that of γ-TiAl substrate [34]. In general, this indicated that the ability of the surface tissues of Cr-Nb to resist plastic deformation, elastic deformation and creep deformation was enhanced after the plasma surface Cr-Nb co-alloying. There was no doubt that it was beneficial to the resistance of γ-TiAl to fretting wear.

Fig.7 showed the hardness, elastic modus (a) and H/E, H^3/E^2 (b) of γ-TiAl before and after plasma surface Cr-Nb co-alloying. As shown in Fig. 7(a), the surface nano-hardness and modulus of elasticity of γ-TiAl were significantly increased after plasma surface Cr-Nb co-alloying. The surface nanohardness (H) of γ-TiAl increased from 5.65 GPa to 11.61 GPa. In addition, the elasticity modulus (E) of γ-TiAl increased from 167.75 GPa to 194.12 GPa after plasma surface Cr-Nb co-alloying. As shown in Fig. 7 (b), H/E and H^3/E^2 of γ-TiAl matrix were 3.37 and 0.64, respectively. H/E and H^3/E^2 of Cr-Nb co-alloying coating increased to 5.98 and 4.15, respectively. It indicated that the plastic deformation resistance and elastic strain to failure of γ-TiAl were enhanced obviously after Cr-Nb co-alloying, which benefitted to improve the wear resistance.

3.3 Fretting Wear Behavior

Fig. 8 showed the fretting friction coefficient change of γ-TiAl before and after plasma surface Cr-Nb co-alloying with the increasing of cycles. In the initial fretting stage (Region A), the friction coefficient was low due to the presence of the surface contamination layer. After 2000 cycles, the friction coefficient of Cr-Nb alloyed specimen began to stabilize. However, it took 5000 cycles that the friction coefficient of γ-TiAl began to stabilize. In the stage of friction stabilization (Region C and D), the friction coefficient of Cr-Nb alloyed specimen was around 0.8, which was lower than 0.9 of γ-TiAl substrate. It was mainly attributed to high surface hardness of Cr-Nb alloying coating.

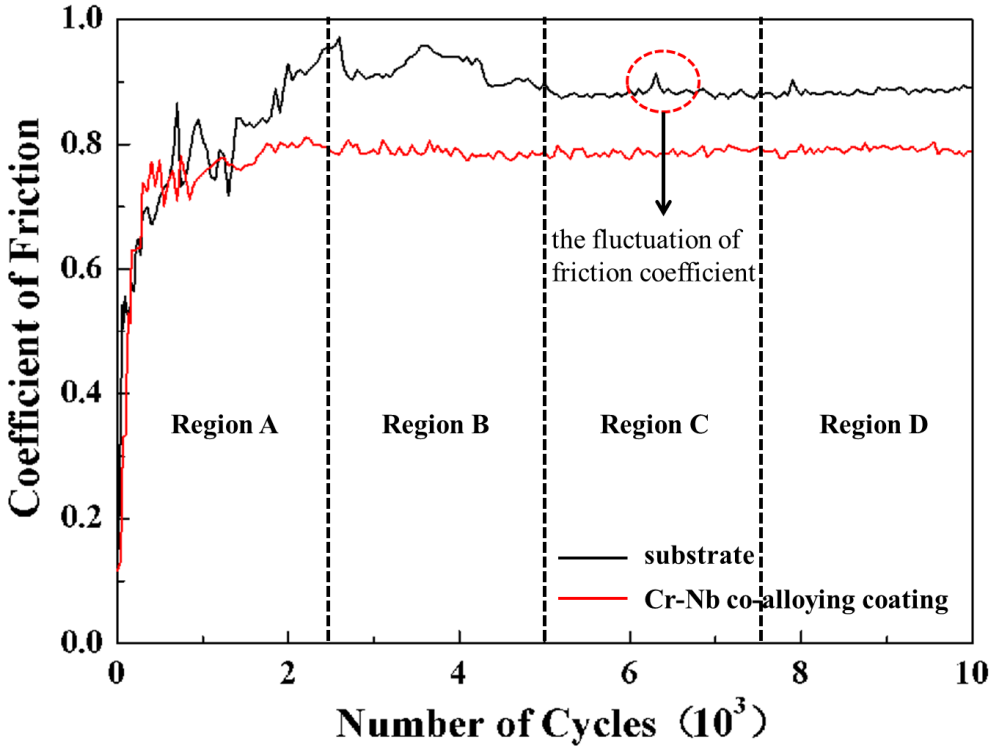

Fig 8 Friction coefficient curves of γ-TiAl before and after plasma surface Cr-Nb co-alloying

It was worth noting that the friction coefficients curve of γ-TiAl substrate showed sharp fluctuations before entering the stable friction stage. The researches on the ball-disc sliding wear of γ-TiAl showed that its wear mechanism was the intense abrasive wear. In the early stage of wear, the friction coefficient fluctuated dramatically due to the continuous formation and accumulation of wear debris [35]. In this study, the friction coefficients of γ-TiAl also showed the sharp fluctuations at the

initial fretting wear stage. It indicated that in addition to poor sliding wear resistance, γ-TiAl still had poor fretting wear resistance. However, the fluctuation of friction coefficient at the initial stage of friction was significantly improved after plasma surface Cr-Nb co-alloying.

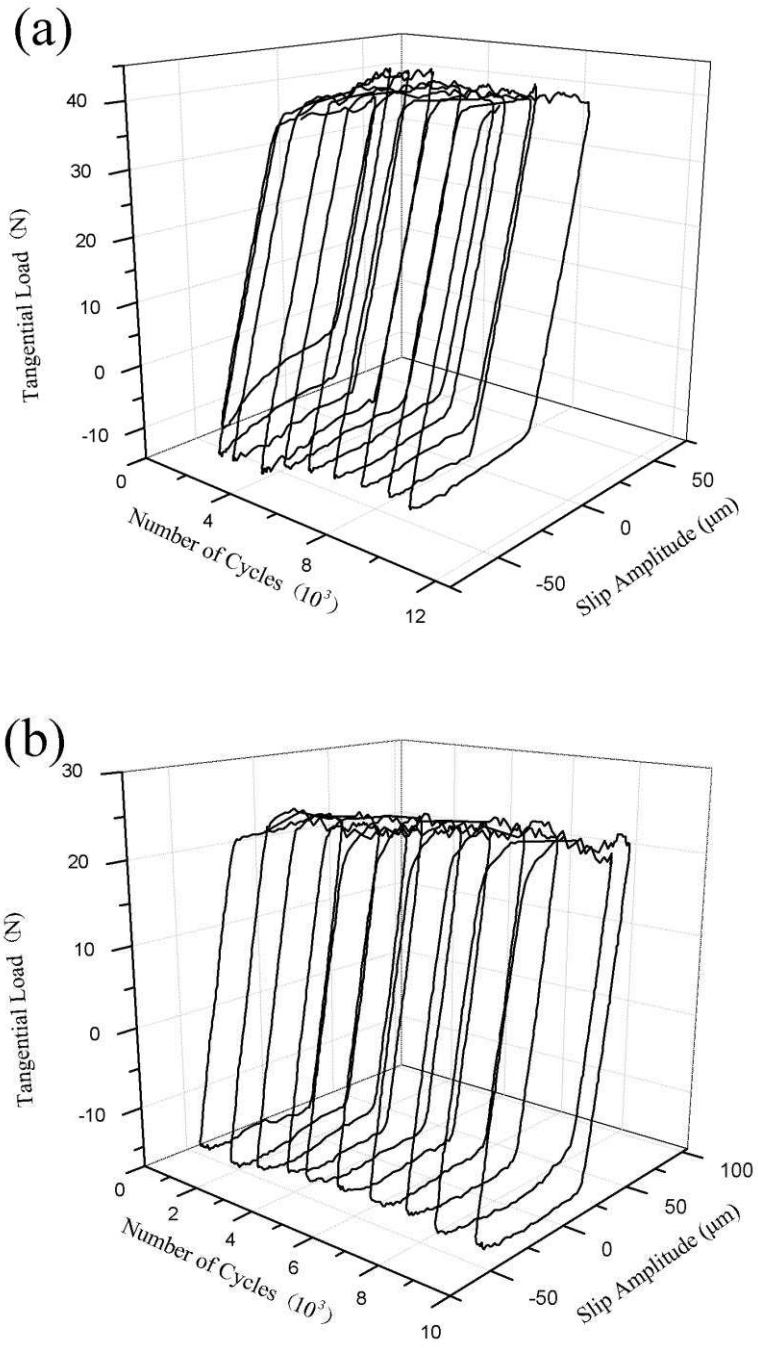

Fig. 9 Fretting loops of uncoated and Cr–Nb-coated γ-TiAl samples recorder under 10000 cycles

Fig. 9 showed the F_t-D curve of γ-TiAl before and after plasma surface Cr-Nb co-alloying with the increasing of cycles. The Ft-D curves were parallelogram, which indicated that the gross slip regime state always in the fretting contact region for the γ-TiAl and Cr-Nb co-alloying coating.

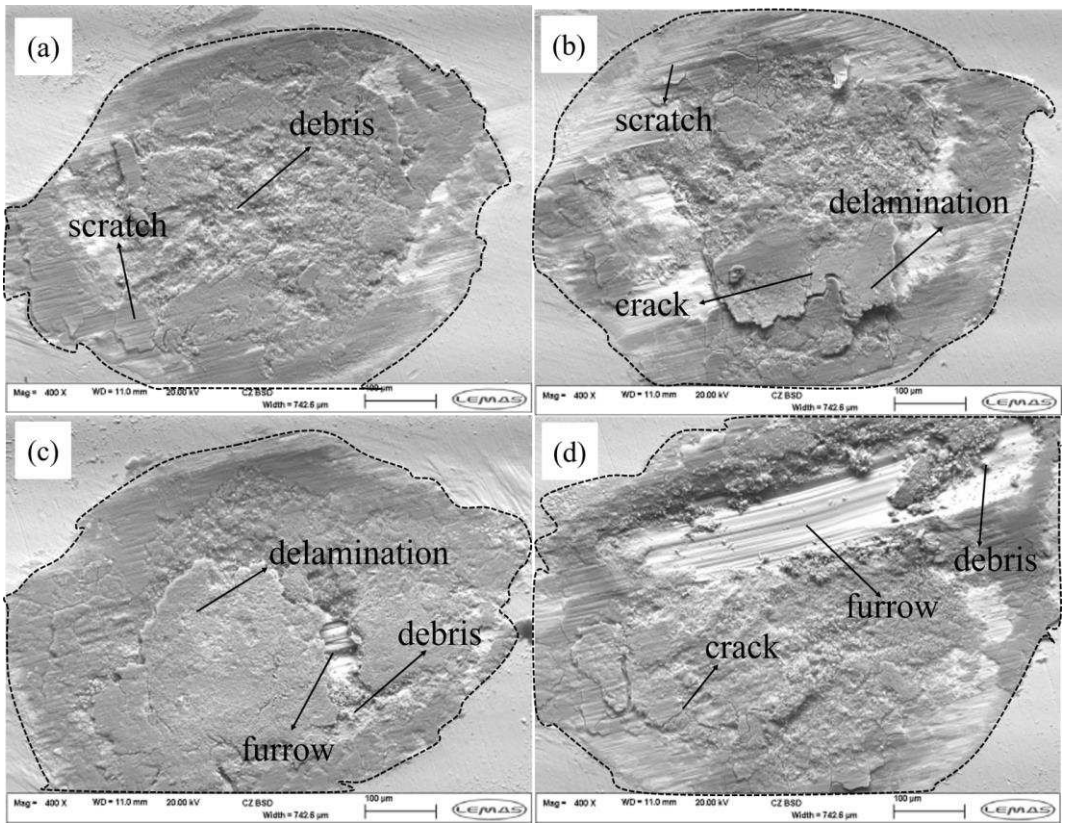

Fig. 10 The fretting wear scar morphology of γ-TiAl

(a) 2500 cycles; (b) 5000 cycles; (c) 7500 cycles; (d) 10000 cycles

Fig. 10 and Fig. 11 respectively showed the fretting wear morphologies and profiles of γ-TiAl with the increasing fretting cycle. As can be seen from Fig. 10(a), when the cycle was 2500 cycles, the wear morphology of γ-TiAl showed a severe abrasive wear in the central area. In the process of fretting wear, a lot of debris was generated in the central area, resulting in abrasive wear. And, it had some scratches in the edge of the wear scar. As the cycle increased to 5000 cycles, mild delamination of γ-TiAl could be observed on the wear scar, and the wear area became bigger than that of 2500 cycles. Moreover, the maximum depth increased from 15 μm of 2500 cycles to 30 μm.

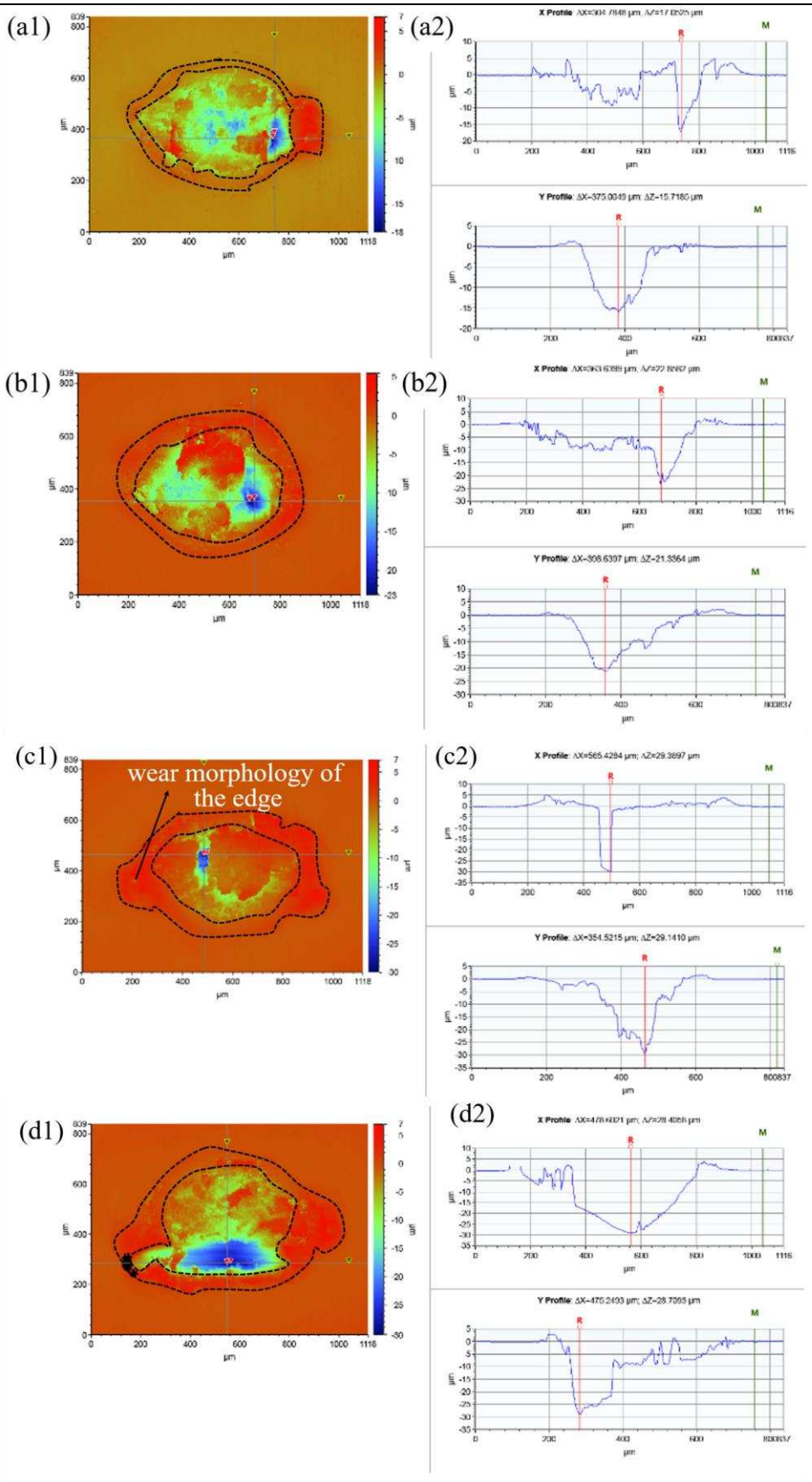

Fig. 11 The fretting wear scar profile curves of γ-TiAl

(a) 2500 cycles; (b) 5000 cycles; (c) 7500 cycles; (d) 10000 cycles

When the cycle increased to 7500 cycles, delamination of γ-TiAl became serious, and it led to a little furrow on the wear scar. When the cycle increased to 10000 cycles, large furrow were observed on the wear scar due to the delamination of γ-TiAl, which made to the average depth continue to increase. Furthermore, as can be seen form Fig.11, the edge of the wear scar was dark red, which indicated that the height of the edge of the wear scar was higher than that of the central area.

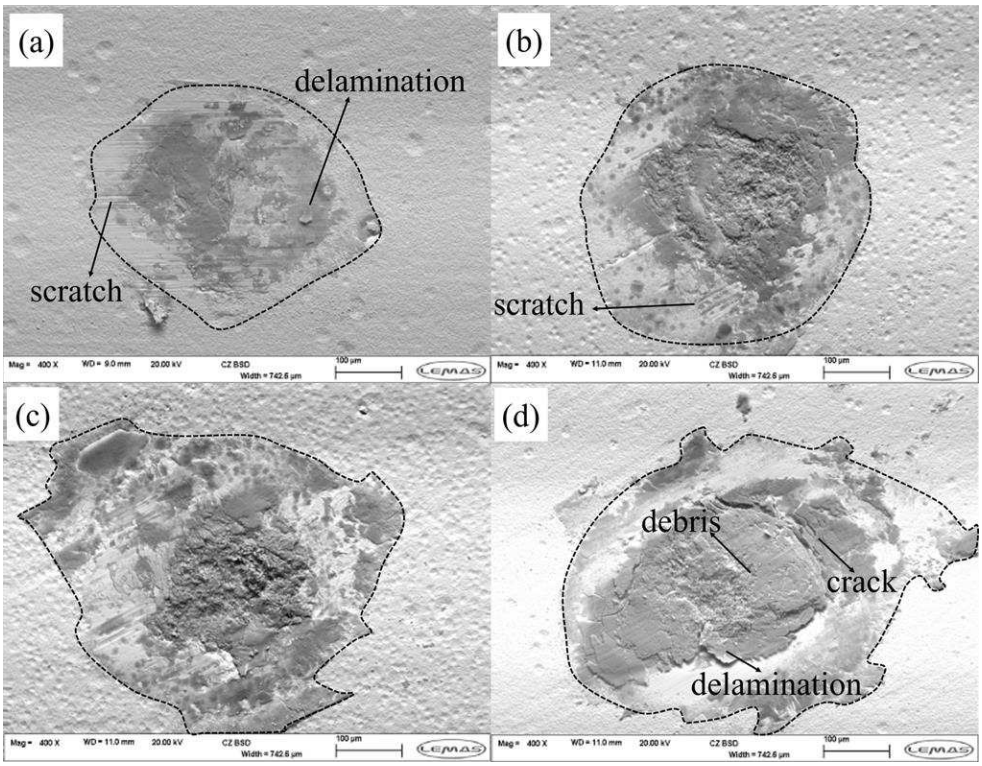

Fig. 12 The fretting wear scar morphology and profile curves of Cr-Nb co-alloying coating

(a) 2500 cycles; (b) 5000 cycles; (c) 7500 cycles; (d) 10000 cycles

Fig. 12 and Fig. 13 respectively showed the fretting wear morphologies and profiles of Cr-Nb co-alloying specimens with the increasing fretting cycle. It could be seen from Fig. 12 that the wear scar area of the Cr-Nb co-alloying coating was smaller than that of γ-TiAl substrate and no obvious wear when the cycle time was 2500 cycles. As the cycle time increased to 5000 cycles, wear of Cr-Nb co-alloying coating in the central area begin to increase, and mild scratch appeared in the edge of the wear scar. When the cycle time increased to 7500 cycles, the wear area continued to increase, and the wear became more severe than that of 5000 cycles.

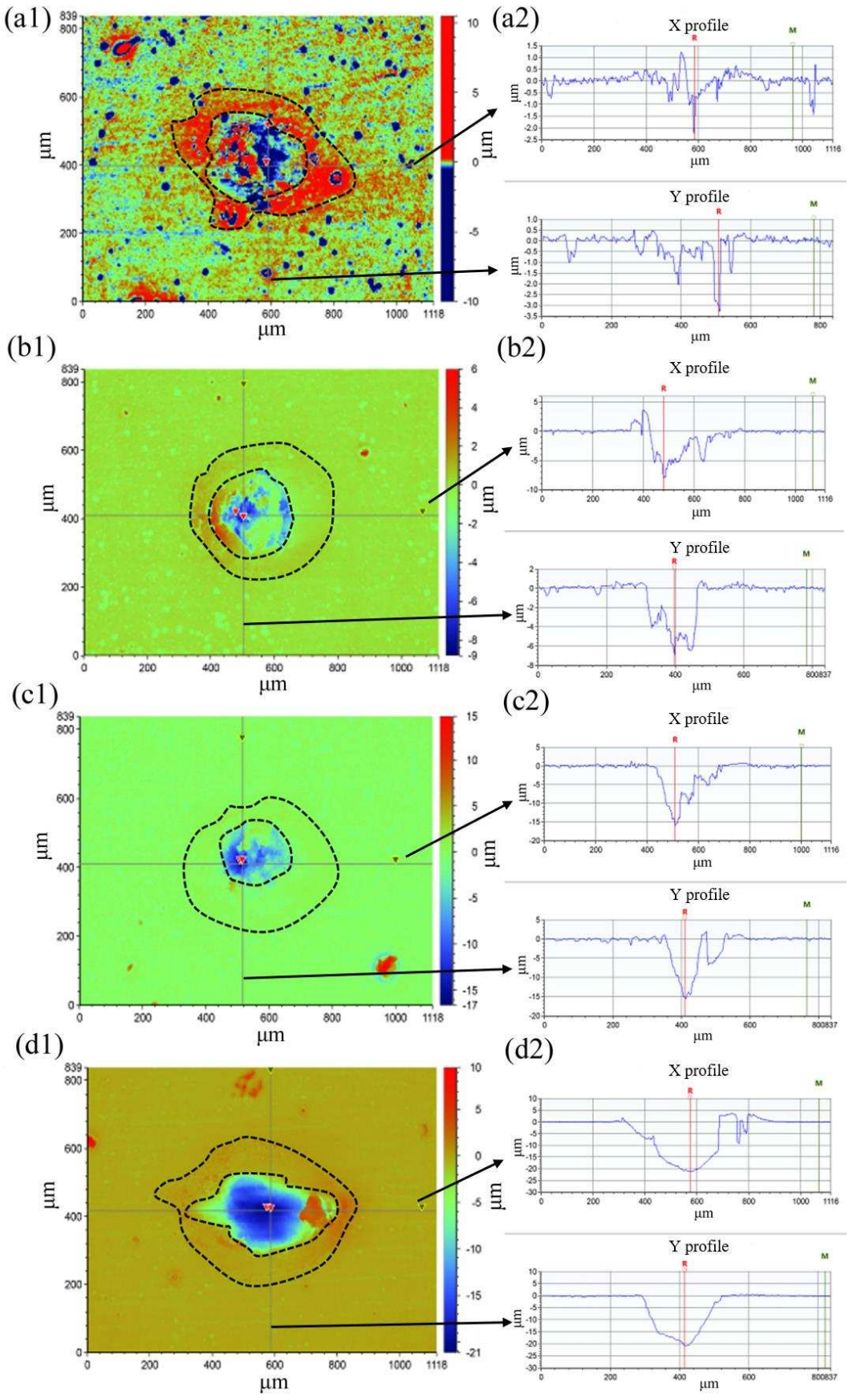

Fig. 13 The fretting wear scar profile curves of Cr-Nb co-alloying coating

(a) 2500 cycles; (b) 5000 cycles; (c) 7500 cycles; (d) 10000 cycles

As the cycle time increased to 10000 cycles, delamination of Cr-Nb co-alloying coating appeared in the central area. However, the height of the edge zone of the Cr-Nb co-alloying coating was lower than the γ-TiAl.

4. Discussion

To investigate the fretting wear mechanism of γ-TiAl before and after Cr-Nb co-alloying coating, the fretting wear tests with different cycles in ambient air condition were conducted. The fretting wear of γ-TiAl showed different stages with the increase of cycles. When the cycle was between 0 and 2500, the wear mechanism was abrasive wear. At the initial stage of wear, wear debris was constantly produced, and the surface of wear scar became rough, which made the friction coefficient fluctuate seriously, as shown in the region A of Fig. 8. However, as the cycle increased to 2500~5000, debris peels off continuously and a third body was formed between the contact surfaces, which acted as solid lubrication, resulting in the reduction of friction coefficient, as shown in the region B of Fig. 8. When the debris formation and overflow reach dynamic equilibrium, fretting entered a stable state, as shown in the region C of Fig. 8. In the meantime, the stress concentration caused by small wear debris caused microcracks on the surface of wear scar, as shown in Fig. 10(b). When the fretting cycles increased to 5000~7500, the further development of microcracks led to delamination and some mild flake-off of γ-TiAl. The flaking of γ-TiAl may be the cause of friction coefficient fluctuation in region C of Fig. 8.

The fretting wear of γ-TiAl after Cr-Nb co-alloying also showed different stages with the increase of cycles compared with γ-TiAl before Cr-Nb co-alloying. However, the wear loss of γ-TiAl after Cr-Nb co-alloying became smaller. When the cycle was between 0 and 2500, there were only slight abrasive wear and little delamination on the wear scar. As the friction cycle increased to 2500~5000, the peels off of debris made the wear increase. But, although the wear loss of the Cr-Nb co-alloying coating increased, it was still lower than that of γ-TiAl substrate. The maximum depth of the wear scar was only 6 μm, far lower than that of the substrate of 30 μm. With the increasing of the cycle time to 5000~7500, the wear continued to increase, and the

maximum depth of the wear scar increased to 20 μm. When the cycle was increased to 7500 and 10000, the stress concentration caused by small wear debris caused obvious microcracks on the surface of wear scar and large delamination was appeared on the wear surface, and the average of wear depth was more than 16μm, which indicated that the exposed area resulting from the delamination may be the Cr-Nb diffusion layer and γ-TiAl substrate.

As can be seen from Fig. 7(a), the hardness and elastic modulus of Cr-Nb co-alloying coating was obvious different from the γ-TiAl substrate. Previous study showed that the different elastoplasticities of the hard coating and soft substrate would cause severe stress concentration in the process of fretting wear, which promoted the nucleation of microcracks at the interface and propagate upward to the surface of Cr-Nb coating [36]. However, the existence of diffusion layer could solve this problem. Cr, Nb, Ti, and Al showed gradient distribution in the diffusion layer. The Cr-Nb co-alloying coating was metallurgical bonded to the γ-TiAl substrate. The low internal stress and high adhesive strength were the main advantages for the fatigue resistance of Cr-Nb co-alloying coating. The existence of the diffusion layer could significantly reduce the crack growth rate which due to the inhomogeneity effect, thus improving the fatigue resistance of the Cr-Nb co-alloying coating. Therefore, a lot of cracks and delamination were not observed until the friction cycle increased to 10000 times. In the meantime, with higher hardness and elastic modulus than the γ-TiAl substrate, the Cr-Nb co-alloying coating had better resistance to the initial contact stress, resulting in a smaller contact area under the same applied load and reduced friction coefficient. As shown in Fig. 8, the friction coefficient (friction coefficient: 0.8) between the γ-TiAl surface after Cr-Nb co-alloying and the friction ball was slightly reduced compared with that of γ-TiAl substrate (friction coefficient: 0.9).

Furthermore, the microplastic deformation occurred on the surface of the two specimens in the process of fretting wear, which could be seen from the fretting loops shown in Fig. 9(a) and (b). Nano-mechanical characterization indicated that the microplastic deformation resistance of bare γ-TiAl was much lower than γ-TiAl after

Cr-Nb co-alloying, which explained why delamination phenomenon occurred earlier on the bare γ-TiAl. Moreover, the hardness and elastic modulus ratio also constitutes a parameter for the γ-TiAl wear resistance measurements [37]. The H/E was the resistance of elastic strain to failure and the H^3/E^2 represented the resistance to plastic deformation of the γ-TiAl before and after Cr-Nb co-alloying [37,38]. As shown in Fig. 7, H/E and H^3/E^2 of Cr-Nb co-alloying coating were significantly higher than that of the γ-TiAl. The Cr-Nb co-alloying coating with high resistance to plastic deformation had strong deformation adaptability and ability to absorb deformation energy, which was not easy to produce cracks or delamination in the process of fretting wear. So until the friction cycles increased to 7500~10000, the wear scar of γ-TiAl after Cr-Nb co-alloying did not appear delamination compared with the γ-TiAl substrate. In addition, the plastic deformation resistance of the substrate was low, which made the γ-TiAl substrate to push away and accumulate on the side during fretting wear, and greatly enlarged the area of wear scar, as shown in Fig. 11 (a), (b), (c) and (d). However, for the wear scar of the Cr-Nb co-alloying coating (Fig. 12 (a), (b), (c) and (d)), the height of the edge zone was basically the same as that of the non-wear zone, which also indicated the better plastic deformation than γ-TiAl substrate.

At the point of the engineering application, on the basis of the equipotential hollow cathode effect, plasma alloying technology could sputter Cr and Nb elements with high melting point from the target material at a temperature lower than that of traditional technology. Furthermore, by means of unequal potential cathode effect, Cr and Nb could be diffused into the matrix, thus effectively improving both the high temperature oxidation resistance and fretting wear resistance of γ-TiAl. In addition, the plasma had the characteristics of full coverage and could maintain the required size accuracy after plasma alloying, so that the technology may be applied to complex parts such as engine blades, which provided a new technical support for improving the fretting wear resistance of aero engine parts.

5. Conclusions

In this study, surface Cr-Nb co-alloying was realized on γ-TiAl based double glow plasma hollow cathode discharge. The effect of surface Cr-Nb co-alloying on fretting friction behavior of γ-TiAl was systematically analyzed based on microstructure, nano-mechanical characterization and fretting wear of γ-TiAl before and after plasma surface Cr-Nb co-alloying. The following conclusions were drawn:

(1) Intense hollow cathode sputtering resulted in a huge component bias between Cr-Nb target and the surface of γ-TiAl. Cr_2Nb intermetallic compounds were formed under the surface, which led to the chrome-depletion of the surface. In the meantime, an inter-diffusion behavior of Cr, Nb and Ti, Al occurred and resulted to an interdiffusion formed. It was the key reason for the anti-fretting wear performance improvement of γ-TiAl after plasma surface Cr-Nb co-alloying.

(2) After plasma surface Cr-Nb co-alloying, the surface nanohardness (H) of γ-TiAl increased from 5.65 GPa to 11.61 GPa. The H^3/E^2 increased from 0.64 to 4.15, which was approximately 6.48 times than that of γ-TiAl. It indicated that plasma surface Cr-Nb co-alloying improved the plastic deformation and fretting fatigue resistance of γ-TiAl, which was also beneficial to the anti-fretting wear performance improvement of γ-TiAl.

(3) After Cr-Nb plasma alloying, the increase of hardness and plastic deformation resistance reduced the friction coefficient and fluctuation of the friction between γ-TiAl and Si_3N_4 ball. In different cycles, the surface scar area and maximum depth of γ-TiAl after Cr-Nb co-alloying were significantly lower than that before alloying, which significantly reduced the wear loss of γ-TiAl during fretting wear.

(4) With the increase of friction cycle, the friction process of both γ-TiAl before and after Cr-Nb co-alloying could be divided into the formation of debris, flaking, formation of crack, delamination. The high hardness, resistance to plastic deformation and fatigue resistance of γ-TiAl after Cr-Nb co-alloying could inhibit the formation of debris and delamination during friction test, resulting in lower wear loss.

(5) This study proved that plasma surface alloying was an effective way to

improve the fretting wear performance of γ-TiAl. In this study, the effect of plasma Cr-Nb co-alloying on the fretting wear behavior of alloy was tested and analyzed at a low frequency (5Hz). It was well-know that the turbine spindle speed in the third and fourth generation engine was as high as 13000-15000. Blades made of γ-TiAl faced the risk of severe high-frequency fretting wear at this speed. In order to further estimate the effect of Cr-Nb co-alloying on γ-TiAl, Further research was necessary for the fretting wear behavior study under high frequency conditions.

Acknowledgement

This project was supported by Natural Science Foundation for Excellent Young Scientists of Jiangsu Province, China (Grant No. BK20180068), China Postdoctoral Science Foundation funded project (Grant No. 2018M630555), the Fundamental Research Funds for the Central Universities, China (Grant No. NS2018039), Opening Project of Materials Preparation and Protection for Harsh Environment Key Laboratory of Ministry of Industry and Information Technology (Grant No. NJ2018009), Opening Project of Aero-engine Thermal Environment and Structure Key Laboratory of Ministry of Industry and Information Technology, China (Grant No. CEPE2019005).

References

[1] J. Cheng, Y. Yuan, L. Fu, L. Fei, Z. Qiao, J. Li, J. Yang, W. Liu, Effect of TiB2 on dry-sliding tribological properties of TiAl intermetallics, Tribol. Int. 62 (2013) 91–99.

[2] MIYOSHI, Kazuhisa, LERCH, A. Bradley, DRAPER, L. Susan, Fretting wear of Ti-48Al-2Cr-2Nb, Tribol. Int. 36 (2003) 145–153.

[3] J. Cheng, L. Fei, S. Zhu, Y. Yuan, Z. Qiao, J. Yang, Electrochemical corrosion and tribological evaluation of TiAl alloy for marine application, Tribol. Int. 115 (2017) 483–492.

[4] N. Palaniappan, I.S. Cole, F. Caballero-Briones, S. Manickam, C. Lal, J. Sathiskumar, Neodymium-decorated graphene oxide as a corrosion barrier layer on Ti6Al4V alloy in acidic medium, RSC Adv. 9 (2019) 8537–8545.

[5] K. Zhang, T. Zhang, X. Zhang, L. Song, Corrosion resistance and interfacial morphologies of a high Nb-containing TiAl alloy with and without thermal barrier coatings in molten salts, 156 (2019) 139–146.

[6] F.B. Wang, G. Wang, L. Ji, D.C. Zeng, E ff ects of di ff erent temperatures on

the lamellar structure evolution in γ - TiAl alloys : A phase- fi eld study, 164 (2019) 22–30.

[7] X.J. Zhang, Q. Li, S.Y. Zhao, C.X. Gao, L. Wang, J. Zhang, Improvement in the oxidation resistance of a g -TiAl-based alloy by sol – gel derived Al 2 O 3 film, 255 (2008) 1860–1864. doi:10.1016/j.apsusc.2008.06.041.

[8] M. Yoshihara, Y. Kim, Oxidation behavior of gamma alloys designed for high temperature applications, 13 (2005) 952–958. doi:10.1016/j.intermet.2004.12.007.

[9] M.R. Shanabarger, Comparative study of the initial oxidation behavior of a series of titanium – aluminum alloys, (1998) 179–186.

[10] Y. Mishin, C. Herzig, OVERVIEW NO . 136 DIFFUSION IN THE Ti ± Al SYSTEM, 48 (2000).

[11] J. Qiu, Z. Fu, B. Liu, Y. Liu, J. Yan, D. Pan, W. Zhang, I. Baker, Effects of niobium particles on the wear behavior of powder metallurgical γ- TiAl alloy in different environments, 435 (2019).

[12] M. Mitoraj, E.M. Godlewska, Intermetallics Oxidation of Ti e 46Al e 8Ta in air at 700 C and 800 C under thermal cycling conditions, 34 (2013).

[13] 18---Isothermal oxidation behavior and microstructure of plasma surface Ta coating on ÃŽÂ^3-TiAl.pdf, (n.d.).

[14] T. Popela, J. Kubásek, J. Maixner, P. Novák, Intermetallics Comparison of Nb- and Ta-effectiveness for improvement of the cyclic oxidation resistance of TiAl-based intermetallics, 19 (2011) 493–501. doi:10.1016/j.intermet.2010.11.025.

[15] P. Raluca, S. Friedle, M. Schütze, Intermetallics Oxidation protection of g -TiAl-based alloys e A review, 56 (2015).

[16] A. Brotzu, F. Felli, D. Pilone, Intermetallics Effect of alloying elements on the behaviour of TiAl-based alloys, 54 (2014) 176–180.

[17] Y.B., Zhao, S.Z., Zhang, C.J., Zhang, P., Lin, Z.P., Hou, Microstructural evolution of hot-forged high Nb containing TiAl alloy during high temperature tension, (n.d.).

[18] D. Pilone, F. Felli, A. Brotzu, Intermetallics High temperature oxidation behaviour of TiAl e Cr e Nb e Mo alloys, 43 (2013) 131–137.

[19] J.P. Lin, L.L. Zhao, G.Y. Li, L.Q. Zhang, X.P. Song, F. Ye, G.L. Chen, Intermetallics Effect of Nb on oxidation behavior of high Nb containing TiAl alloys, 19 (2011) 131–136. doi:10.1016/j.intermet.2010.08.029.

[20] H. Saage, A.J. Huang, D. Hu, M.H. Loretto, X. Wu, Intermetallics Microstructures and tensile properties of massively transformed and aged Ti46Al8Nb and Ti46Al8Ta alloys, 17 (2009) 32–38. doi:10.1016/j.intermet.2008.09.006.

[21] X. Lu, X.B. He, B. Zhang, X.H. Qu, L. Zhang, Z.X. Guo, J.J. Tian, High-temperature oxidation behavior of TiAl-based alloys fabricated by spark plasma sintering, 478 (2009) 220–225. doi:10.1016/j.jallcom.2008.11.134.

[22] A. Ismaeel, C. Wang, Effect of Nb additions on microstructure and properties of γ -TiAl based alloys fabricated by selective laser melting, 29 (2019).

doi:10.1016/S1003-6326(19)65009-0.

[23] F. Wang, Z. Tang, W. Wu, Effect of chromium on the oxidation resistance of TiAl intermetallics, Oxid. Met. 48 (n.d.) 381–390.

[24] D. Wei, F. Li, P. Zhang, X. Chen, F. Ding, Z. Yao, Sliding wear behaviour of Ni-Cr alloying on Ti6Al4V based on double-glow plasma surface metallurgy technology Sliding wear behaviour of Ni-Cr alloying on Ti6Al4V based on double- glow plasma surface metallurgy technology, (2018) 0–14.

[25] D. Wei, P. Zhang, Z. Yao, X. Wei, J. Zhou, X. Chen, P. Zhang, Z. Yao, X. Wei, J. Zhou, X. Chen, D. Wei, P. Zhang, Z. Yao, X. Wei, J. Zhou, X. Chen, Oxidation behaviour of plasma surface alloying on Ti6Al4V alloy Oxidation behaviour of plasma surface alloying on Ti6Al4V alloy, 0844 (2016). doi:10.1179/1743294415Y.0000000095.

[26] X. Zhong, B.H. Fang, W.N. Zheng, C.Z. Wang, B. Tang, A novel plasma surface metallurgy: Xu-Tec process, Surf. Coat. Technol. 43–44 (n.d.) 1065–1073.

[27] M. Ciavarella, G. Demelio, A review of analytical aspects of fretting fatigue, with extension to damage parameters, and application to dovetail joints ☆, Int. J. Solids Struct. 38 (2001) 1791–1811.

[28] X. Liang, Z. Liu, B. Wang, State-of-the-art of surface integrity induced by tool wear effects in machining process of titanium and nickel alloys : A review, 132 (2019) 150–181.

[29] X.U. Xiaojun, X.U. Wei, EDERVEEN, F. Hipgrave, V. Der Zwaag, Sybrand, Design of low hardness abrasion resistant steels, Wear. 301 (2013) 89–93.

[30] X. Qiu, X. Wei, X. Xu, W. Xu, M. Zhu, Tribology International Dependence of fretting wear resistance on microstructural features of alloyed steels, Tribiology Int. 137 (2019) 39–45. doi:10.1016/j.triboint.2019.04.028.

[31] D. Wei, P. Zhang, Z. Yao, X. Chen, F. Li, Double glow plasma surface Cr-Ni alloying of Ti6Al4V alloys: Mechanical properties and impact of preparing process on the substrate, Vacuum. (2018). doi:10.1016/j.vacuum.2018.05.049.

[32] X. Chen, P. Zhang, D. Wei, H. Zhao, X. Wei, F. Ding, Tribological Behavior of Aluminum Slurry Coating on 300M Steel, J. Mater. Eng. Perform. 26 (2017) 3719–3727. doi:10.1007/s11665-017-2820-6.

[33] Y. Ma, G.J. Peng, D.H. Wen, T.H. Zhang, Materials Science & Engineering A Nanoindentation creep behavior in a CoCrFeCuNi high-entropy alloy fi lm with two different structure states, 621 (2015) 111–117. doi:10.1016/j.msea.2014.10.065.

[34] S. Anand Kumar, S. Ganesh Sundara Raman, T.S.N. Sankara Narayanan, R. Gnanamoorthy, Influence of counterbody material on fretting wear behaviour of surface mechanical attrition treated Ti-6Al-4V, Tribol. Int. 57 (2013) 107–114. doi:10.1016/j.triboint.2012.07.021.

[35] Z. Iqbal, N. Merah, S. Nouari, A. Rahman, N. Al-aqeeli, Tribology International Investigation of wear characteristics of spark plasma sintered W-25wt % Re alloy and W-25wt % Re-3 . 2wt % HfC composite, Tribol. Int. 116 (2017) 129–137. doi:10.1016/j.triboint.2017.06.042.

[36] X. Shi, T.W. Liskiewicz, B.D. Beake, Z. Sun, J. Chen, Applied Surface Science Fretting wear behavior of graphite-like carbon fi lms with bias-graded deposition, 494 (2019) 929–940.

[37] A. Leyland, A. Matthews, On the significance of the H / E ratio in wear control: a nanocomposite coating approach to optimised tribological behaviour, Wear. 246 (2000) 1–11.

[38] B.Z. Duan, P.Z. Zhang, X.F. Wei, L. Wang, D.B. Wei, D.D. Zhen, Effects of elements W and C on microstructure and wear property of Î^3-TiAl surface alloying layer, Surf. Eng. 31 (2014) 942–948.